

## Assessment of methods to analyze chip and burr formation in micro drilling

Sonja Kieren-Ehse<sup>1</sup>, Felix Zell<sup>1</sup>, Benjamin Kirsch<sup>1</sup>, Jan C. Aurich<sup>1</sup>

<sup>1</sup>*Institute for Manufacturing Technology and Production Systems, RPTU Kaiserslautern, Gottlieb-Daimler-Str., 67663 Kaiserslautern, Germany*

*sonja.kieren-ehses@rptu.de*

---

### Abstract

Micro drilling is used in a wide variety of applications such as medical technology, electronics, micromechanics and microfluidics. It is characterized by its high geometric precision, the excellent surface quality, and the ability to machine a wide range of different materials compared to other processes to produce micro holes. However, burr formation is a challenge in micro drilling because the functionality of the components can be impaired by the burr formation. Subsequent deburring of the holes is often not possible due to the small dimensions. For this reason, burr formation must be prevented or minimized during the manufacturing of the components. Possible adjustment variables for reducing burr formation include the cutting parameters, the tool geometry, the use of tool coatings or the application of metalworking fluids. To be able to control burr formation, it is necessary to analyze the burr and chip formation. Possible measurands are the burr formation at the hole entry and exit, the surface roughness of the hole wall, and the chips. However, the analysis of burr formation at the micro holes represents a challenge due to the small structure sizes. The aim of this publication is the selection of suitable analysis methods and their subsequent application to micro holes with a diameter of 100  $\mu\text{m}$ . Analysis techniques used in literature are compared and evaluated regarding their applicability for micro holes with diameters  $\leq 100 \mu\text{m}$ .

micro drilling, burr formation, measurement

---

### 1. Introduction

The formation of burrs during micro drilling can lead to functional impairment of the components. The small dimensional size of the holes often precludes subsequent deburring. Therefore, it is essential to prevent or minimize burr formation during the manufacturing process. To optimize burr formation, it is necessary to analyze the burr and chip formation – which is challenging at the given small dimensions.

Various methods are used in the literature to evaluate the burr formation of micro holes. One measurand that is evaluated is the burr height. Often either the maximum burr height is determined [1] or the burr height is measured at various points and then the average value is calculated [2]–[4]. Other measurands to characterize the burr are the burr thickness [4], [5] or the burr type [4], [6].

In addition to the burr that remains on the hole after machining, the evaluation of the chip formation is also important, as the chip formation has a direct influence on the burr formation. To evaluate chip formation, the chips formed during the process can be examined [1], [7], [8]. However, due to the small size of the chips when applying very small micro drills, collecting the chips during the process is very challenging – research on examination of chips is hardly available. An indirect method for evaluating chip formation is the evaluation of process forces. Often the thrust force was evaluated (e.g. [9], [10]), rarely the torque (e.g. [2], [11]).

This paper shows different options for the evaluation of micro holes with a diameter of 100  $\mu\text{m}$  and compares them regarding their applicability for small micro holes.

### 2. Experimental setup

#### 2.1. Experimental setup, tools, and workpiece material

The experiments were carried out on the micro milling center [12] developed at our institute. Single-edged cemented carbide micro drills (manufacturer: Prestera<sup>1</sup>) were used for the micro drilling tests. The tools had a diameter of 100  $\mu\text{m}$ , a drill-point angle of 120°, a helix angle of 0°, and a flute length of 700  $\mu\text{m}$ . The workpiece material used was brass (CuZn39Pb2) with a size of 10 mm x 20 mm x 3 mm.

#### 2.2 Process parameters

The feed per tooth was varied at two levels (0.5  $\mu\text{m}$  and 1  $\mu\text{m}$ ). The parameters spindle speed ( $n = 30,000 \text{ min}^{-1}$ ) and hole depth (150  $\mu\text{m}$ ) were kept constant. The final drilling depth was drilled in four steps. First, a depth of 30  $\mu\text{m}$  was drilled so that the drill tip had completely entered the workpiece. The final drilling depth of 150  $\mu\text{m}$  was subsequently drilled in three steps of 50  $\mu\text{m}$  each. In between these steps, the micro drill was retracted above the surface to remove the chips out of the hole. The total feed travel of 180  $\mu\text{m}$  is thus composed of the drilling depth of 150  $\mu\text{m}$  and the immersion length of the micro drill tip, which has a length of 30  $\mu\text{m}$ . For each parameter combination five holes were drilled. During the tests, the process forces were recorded with a dynamometer (MiniDyn Typ 9119AA1, Kistler<sup>1</sup>).

### 3. Measurement systems and evaluation methods

To analyze the burrs and the diameter of the drilled holes different measurement systems and evaluation methods were used. It is important that the measurement systems have a sufficiently high resolution. Before evaluation, the workpiece

was cleaned in an ultrasonic bath with isopropanol to remove loose chips.

The holes were recorded with two different microscopes:

- confocal microscope: Nanofocus<sup>1</sup> OEM microscope, 60x objective lens with a numerical aperture of 0.9, measuring field: 268  $\mu\text{m}$  x 268  $\mu\text{m}$
- light microscope: ZEISS<sup>1</sup> AxioScope 5 Mat, 50x objective lens, software: ZEN core

### 3.1 Diameter

The diameter was evaluated using the measuring software of the light microscope (ZEN core), the evaluation of the confocal images with the MountainsMap software by Digital surf<sup>1</sup> and the evaluation of the height information of the confocal images was done in Matlab:

When using the light microscope, first the surface of the sample was focused and then an image was taken with the 50x objective lens. Then the user placed a circle in the software ZEN core into the hole and the diameter was then derived (see Figure 1 a).

The evaluation of the hole diameter in the MountainsMap software was done analogous to the evaluation in [11]. The user placed horizontal and vertical measurement lines in the hole (see Figure 1 b). Subsequently, the mean value was calculated out of these two lengths.

For the evaluation in Matlab, first the confocal microscope image was aligned in the MountainsMap software. Then the unmeasured points of the hole (it was not measured to the bottom of the hole) were set to a value underneath the original surface (green surface - Figure 1 b). The height profile was then exported as a .txt file and imported into Matlab. A binary image of the hole was generated, in which the points that were not originally measured are shown as white pixels (see Figure 1 c) – binary image). In the next step, a best fit circle was calculated from which the diameter of the hole was determined.

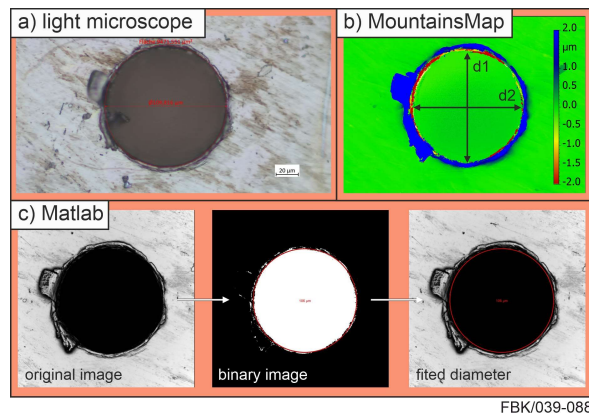


**Figure 1:** Various evaluation methods for determining the hole diameter a) Light microscope b) MountainsMap software c) Image processing in Matlab

### 3.2 Burr formation

Two different evaluation methods were compared to evaluate the burr formation. These were used to determine three different burr measurands:

The evaluation of burr width with the software MountainsMap was done analogous to the procedure in [11] (see Figure 2 a). The burr width was determined by measuring the burr width at two different locations that indicate the uniform burr around the hole. Then the mean value was calculated. Larger burrs were ignored and only the uniform burr was considered.

The burr height was evaluated using the software MountainsMap, whereby the surface parameter Sp (maximum peak height) was calculated that corresponds to the maximum burr height. In addition, the hole was divided into four quadrants

and Sp was determined for each quadrant. The mean value was then calculated out of these four values.

The burr area was determined in Matlab using image processing. Prior to this, the confocal microscope image (see Figure 2 b) was exported as a .txt file using the MountainsMap software. Subsequently, the data were imported into Matlab. The surface was determined and all values above this surface were converted into black pixels. The resulting binary image shows the burr (see Figure 2 b). The burr area in  $\mu\text{m}^2$  is determined by counting the black pixels in the binary image.

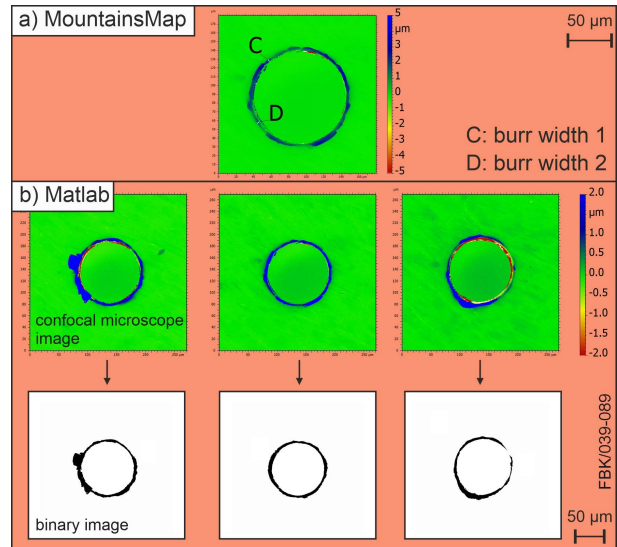


**Figure 2:** Various evaluation methods for determining burr formation a) MountainsMap software b) Image processing in Matlab

### 3.3 Chips

The chips were collected during the process using a container that was placed underneath the workpiece. The chips were recorded using the light microscope.

### 3.4 Forces

The recorded forces were first filtered with a high-pass (1 Hz) and low-pass (6 000 Hz) filter in the software NI<sup>1</sup> DIAdem. A moving average (root mean square) was then calculated. Next the feed force  $F_f$  and the cutting force  $F_c$  were exported as a .csv file and imported into Matlab.

In Matlab, first the mean value of the force was determined for each drilling step, whereby only the forces during the feed movement were considered. For the calculation, the first and last 10 % of the feed travel were not considered (see Figure 3). Furthermore, the forces generated during the retraction of the tool were not considered in this calculation. As a further parameter, the maximum force that occurred was determined.

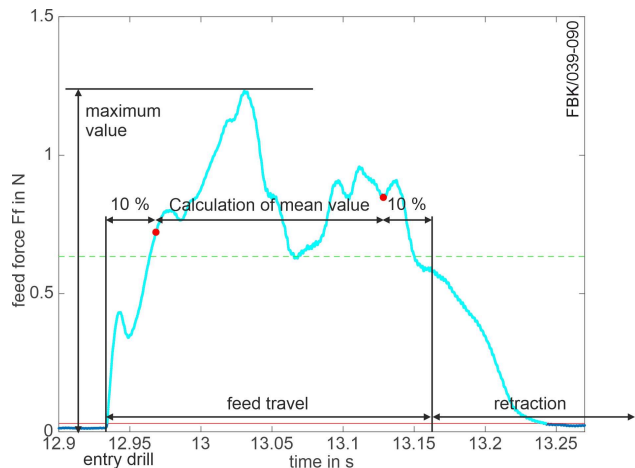


**Figure 3:** Evaluation of the force signal

## 4. Results and discussion

### 4.1 Diameter

Figure 4 shows the measured diameters of the holes depending on the feed per tooth and the evaluation method. The results depend on the considered methods and vary between 101  $\mu\text{m}$  and 110  $\mu\text{m}$ . Looking at the confocal microscope image in Figure 1 b) there are three different colored areas visible: the surface in green, the burr in blue and a red area. The red area is the result of the drift of the micro drill during entering the workpiece. The cause of the drift is probably the lack of centering of the micro drill at the drill entry, resulting in a tool deflection. The drift creates a ring around the hole with a larger diameter than the hole itself and is only a few micrometers deep. This ring is visible as a red area on the confocal microscope images (see Figure 1 b) because it lies below the surface (shown in green). Due to this red circular ring, there are two different diameters that can be measured: the diameter of the inner hole and the diameter at the surface. When using the light microscope, only the diameter at the surface could be measured due to the lack of depth of field. This fact explains the higher diameters measured from light microscope images (see Figure 4). As part of the evaluation in MountainsMap, the innermost points measured in both directions were used to determine the diameter. This is the reason for the lower diameters for this method. Due to the best fit circle determined via image processing in Matlab, these diameters are between those determined with the light microscope and MountainsMap.

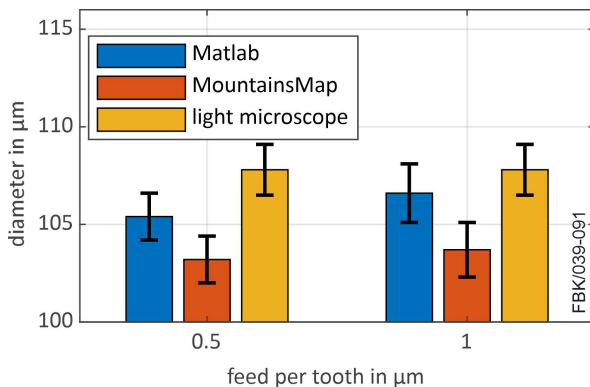


**Figure 4:** Diameter of the micro drilled holes depending on the feed per tooth

As the actual hole diameter is of interest for the application and not the diameter resulting from the drift of the micro drill, the use of the light microscope to evaluate the hole diameter is not an appropriate method.

### 4.2 Burr formation

Figure 5 shows the results of the evaluation of the considered measurands to quantitatively evaluate the burr after micro drilling. All parameters considered show the same trend regarding the influence of the feed per tooth on the burr formation: The burr formation could be reduced by increasing the feed per tooth.

The parameters burr width and burr area both indicate the burr expansion perpendicular to the feed direction of the hole. As the burr width is determined manually in the MountainsMap software, the determination of the total burr area is the more robust parameter.

By determining the parameter  $S_p$ , the burr height can be evaluated. Determining the maximum burr height as well as the average maximum burr height by averaging the  $S_p$  values of the four quadrants of the hole are suitable ways of evaluating the burr height.

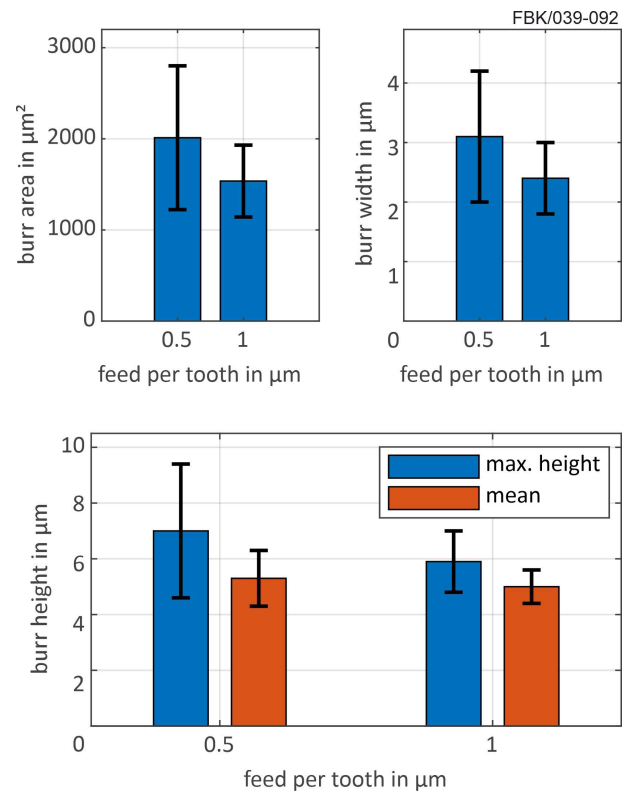


**Figure 5:** Burr formation depending on the feed per tooth

### 4.3 Chips

Figure 6 shows the chips that were collected during the machining of the holes. In the first drilling step helical chips, as shown in Figure 6 left and middle, are formed. In contrast, no more helical chips were formed in the third drilling step. Instead, short chips were produced – see Figure 6 right. This change in chip formation is probably directly related to the process forces depending on the drilling depth. Collecting, preparing and measuring these tiny chips represents a major challenge that must be considered further in future studies.

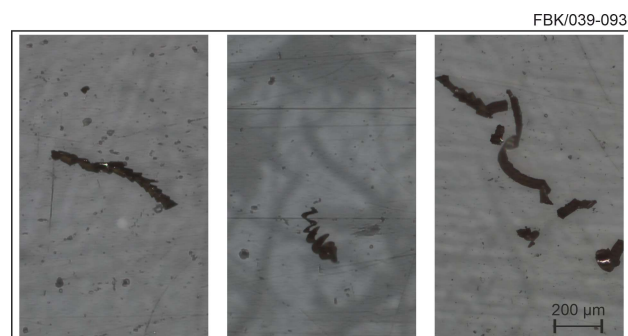


**Figure 6:** Light microscope image of the chips

### 4.4 Forces

Figure 7 shows the maximum as well as the mean forces depending on the feed per tooth. All parameters considered show an increase in forces with increasing feed per tooth.

The maximum forces and especially the maximum feed force  $F_f$  is relevant regarding the low rigidity of micro drills and the associated risk of breakage if the load is too high. The maximum force in feed direction can be used to estimate the risk of tool breakage. A more detailed assessment of the forces occurring during the entire drilling process can be made by looking at the mean values of each drilling step.

The results show that the process forces increase with increasing drilling depth. The reason for this could be the insufficient chip removal from the drill hole. In this case, it is useful to consider the forces for each individual drilling step. If

the forces are the same level for each drilling step, it is sufficient to calculate the mean value for all drilling steps.

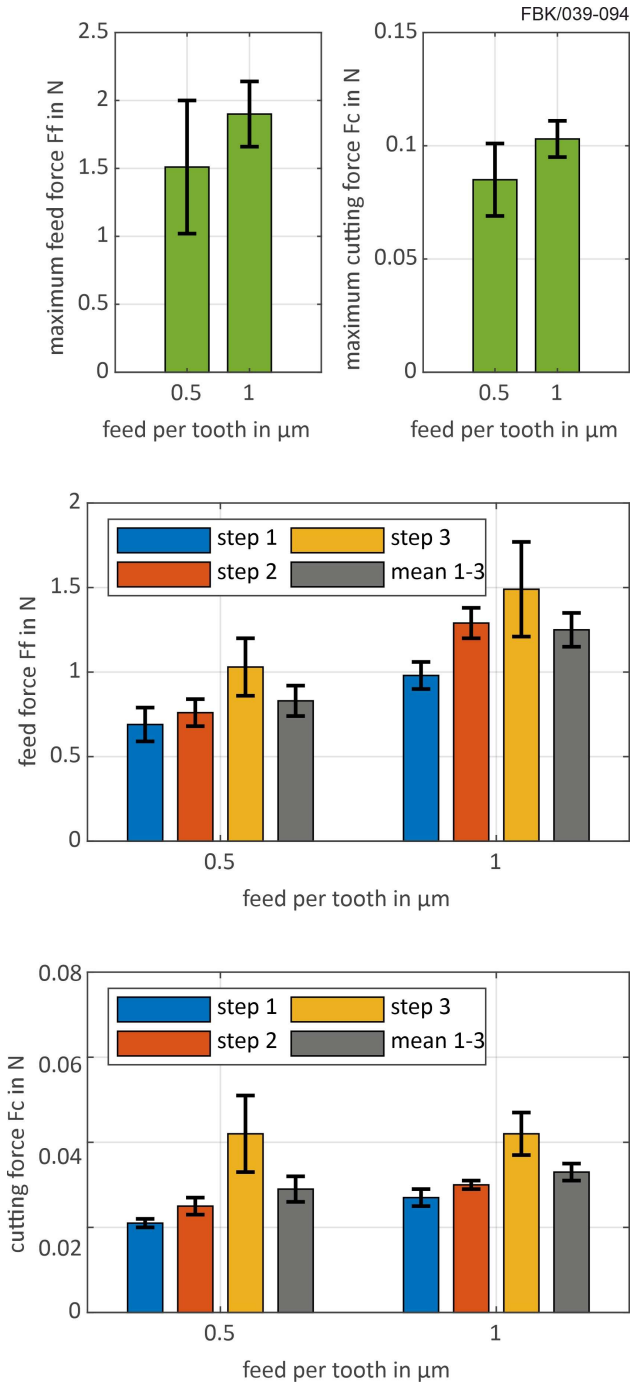


Figure 7: Forces depending on the feed per tooth.

## 5. Conclusion and Outlook

This paper outlines various methods for the analysis of burr and chip formation when micro drilling. To analyze the burrs and the diameter of the drilled holes, a range of measurement systems and evaluation methods were presented. In addition, various options for analyzing the force signals were considered to evaluate the link between process forces and burr/chip formation. The results demonstrate that the influence of the feed per tooth can be determined using the measurands evaluated. Thus, the selection of appropriate measurands is important to identify weak points or optimization possibilities in the process.

In future work, the drift of the drill at the drill entry will be investigated in more detail, as this should be avoided or

minimized. One way of investigating the drift is to evaluate the increase in diameter caused by the drift at the drill entry. In this context, various strategies for the initial immersion of the tool in the material are to be investigated. Furthermore, the evaluation of the forces has demonstrated that the removal of the chips is inadequate. Therefore, further research will be carried out to improve the removal of chips from the hole, for example by optimizing the drilling parameters or optimizing the drill geometry.

## Acknowledgments

Funded by the Deutsche Forschungsgemeinschaft (DFG, German Research Foundation) - project number 453335596.

<sup>1</sup> "Naming of specific manufacturers is done solely for the sake of completeness and does not necessarily imply an endorsement of the named companies nor that the products are necessarily the best for the purpose."

## References

- [1] Prashanth P and Hiremath S S 2023 Experimental and predictive modelling in dry micro-drilling of titanium alloy using Ti-Al-N coated carbide tools *Int J Interact Des Manuf* **17** 553–577
- [2] Abdelhafeez Hassan A, Li M J and Mahmoud S 2020 On Miniature Hole Quality and Tool Wear When Mechanical Drilling of Mild Steel *Arab J Sci Eng* **45** 8917–8929
- [3] Kim D W, Lee Y S, Chu C N and Oh Y T 2006 Prevention of exit burr in microdrilling of metal foils by using a cyanoacrylate adhesive *Int J Adv Manuf Technol* **27** 1071–1076
- [4] Pansari S, Mathew A and Nargundkar A An Investigation of Burr Formation and Cutting Parameter Optimization in Micro-drilling of Brass C-360 Using Image Processing. *Proceedings of the 2nd International Conference on Data Engineering and Communication Technology* **828** 289–302
- [5] Stein J M and Dornfeld D A 1997 Burr Formation in Drilling Miniature Holes *CIRP Annals* **46** 63–66
- [6] Stirn B, Lee K and Dornfeld D A 2001 Burr Formation In Micro-Drilling *Proceedings of the sixteenth annual meeting of the American Society for Precision Engineering*
- [7] Yi S, Li G, Ding S and Mo J 2017 Performance and mechanisms of graphene oxide suspended cutting fluid in the drilling of titanium alloy Ti-6Al-4V *Journal of Manufacturing Processes* **29** 182–193
- [8] Iwata K, Moriwaki T and Hoshi T 1981 Basic Study of High Speed Micro Deep Drilling *CIRP Annals* **30** 27–30
- [9] Zhang H, Zhao S, Wang L, Li C and Hou S 2019 Micro-drilling of AISI 1045 steel using a centering micro-drill *Int J Adv Manuf Technol* **103** 4189–4203
- [10] Azim S, Gangopadhyay S, Mahapatra S S and Mittal R K 2022 Performance evaluation of CrAlN and TiAlN coatings deposited by HiPIMS in micro drilling of a Ni-based superalloy *Surface and Coatings Technology* **449** 128980
- [11] Nam J S, Lee P-H and Lee S W 2011 Experimental characterization of micro-drilling process using nanofluid minimum quantity lubrication *International Journal of Machine Tools and Manufacture* **51** 649–652
- [12] Bohley M, Reichenbach I G, Müller C and Aurich J C 2016 Development of a desktop machine tool for integrated ultra-small micro end mill production and application *Proceedings of the 11th International Conference on Micro Manufacturing*